

Notes on Electrostatic Wire Grids

Kirk T. McDonald

Joseph Henry Laboratories, Princeton University, Princeton, NJ 08544

(March 5, 2003)

1 A Single Grid Plane

(Compare [1] and chap. 3 [2].)

We first consider a single grid plane, as shown in Fig. 1, that consists of wires along the z axis, separated by distance a in the plane $y = 0$.

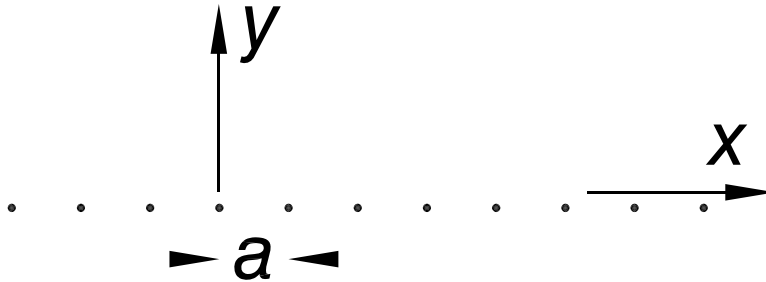


Figure 1: A grid of wires with spacing a in the plane $y = 0$.

The simplest analysis of this grid is when each wire carries charge λ per unit length (and no other charges are present). The form of the potential $V(x, y)$ can be obtained via separation of variables as in Appendix 1, or via conjugate functions [3]. The result is (in Gaussian units)

$$V(x, y) = -\lambda \ln \left[2 \left(\cosh \frac{2\pi y}{a} - \cos \frac{2\pi x}{a} \right) \right]. \quad (1)$$

1.1 Behavior far from the grid

For large $|y|$, $\cosh(2\pi y/a) \rightarrow e^{2\pi|y|/a}/2$, so $V(x, y) \rightarrow -2\pi\lambda|y|/a$. This corresponds to a uniform electric field of strength $\pm 2\pi\lambda/a$ in the y direction, as would also be generated by a uniform sheet of charge of density

$$\sigma = \frac{\lambda}{a}. \quad (2)$$

If this grid is surrounded by other electrodes such that the field for $y > 0$ and far from the grid wires is E_+ , and the field for $y < 0$ is E_- , then Gauss' law tells us that the charge on the wires is related by

$$E_+ - E_- = 4\pi\sigma = 4\pi\frac{\lambda}{a}. \quad (3)$$

1.2 Behavior close to a grid wire

For simplicity, we consider the wire whose center is at $(0,0)$. As shown in eq. (48), the equipotentials close to the wire are circles, with

$$V(x, y) \approx -2\lambda \ln \frac{2\pi r}{a} = 2\lambda \ln \frac{a}{2\pi r}. \quad (4)$$

If the wires have radius $r_0 \ll a$, then the potential of a wire is

$$V_{\text{wire}} \approx 2\lambda \ln \frac{a}{2\pi r_0} = \frac{a(E_+ - E_-)}{2\pi} \ln \frac{a}{2\pi r_0}. \quad (5)$$

Also of interest is the electric field strength at the surface of a wire, which we obtain from eq. (4):

$$E_{r,\text{wire}} = -\frac{dV(r=r_0)}{dr} \approx 2\frac{\lambda}{r_0} = (E_+ - E_-)\frac{a}{2\pi r_0}. \quad (6)$$

Because the potential depends only on r for $r \ll a$, the electric field near the wire is radial and azimuthally symmetric. Hence the surface charge distribution on the wire, $\sigma = E_r/4\pi$, is also azimuthally symmetric.

If the grid is used in a gas-filled particle detector, the field (6) can cause multiplication of the drifting electrons.

2 Grid + Planar Electrodes

The grid considered in sec. 1 can be surrounded by a pair of planar electrodes at $y = -b_1$ and b_2 to form a device whose unit cell is shown in Fig. 2. In general, the potential of the lower cathode of the cell is V_1 , that of the upper cathode is V_2 , and that of the grid is V_0 . We denote the volume $-b_1 < y < 0$ and region 1, and the volume $0 < y < b_2$ as region 2. Then $E_1(x, y)$ is the electric field in region 1, *etc.*

2.1 Grounded Planar Electrodes

In Appendix 2 we analyze the particular case that the planar electrodes are grounded, $V_1 = V_2 = 0$, whose behavior is closely related to that of an isolated grid. A detailed expansion for the potential is given in eqs. (54)-(55). For $|y| \gtrsim a$ the electric field is uniform and the potential varies linearly with y . Close to a wire the equipotentials are circles and the electric field is radial, as shown in Fig. 3.

The potential on the wire (of radius r_0) is now given by

$$V_{\text{wire}} = V_0 \approx \frac{4\pi\lambda b_1 b_2}{ab} + 2\lambda \ln \frac{a}{2\pi r_0} = \frac{4\pi b_1 b_2 (1 + K)}{ab} \lambda \quad (V_1 = V_2 = 0), \quad (7)$$

where

$$K \equiv \frac{ab}{2\pi b_1 b_2} \ln \frac{a}{2\pi r_0}. \quad (8)$$

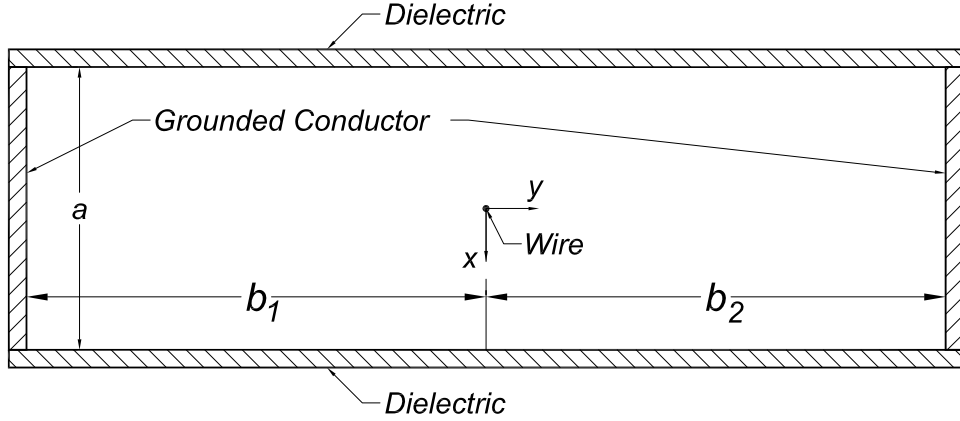


Figure 2: An “electrodeless” drift chamber is a hollow rectangular prism of active area $a \times b (= b_1 + b_2)$ with two opposing faces that are conductors, two faces that are dielectric, and a wire running down the center. During operation of the chamber the dielectric surfaces charge up with positive ions until the electric field is parallel to the dielectric surface. Hence, the interior of this chamber is also a unit cell of a multiwire proportional chamber with planar cathodes.

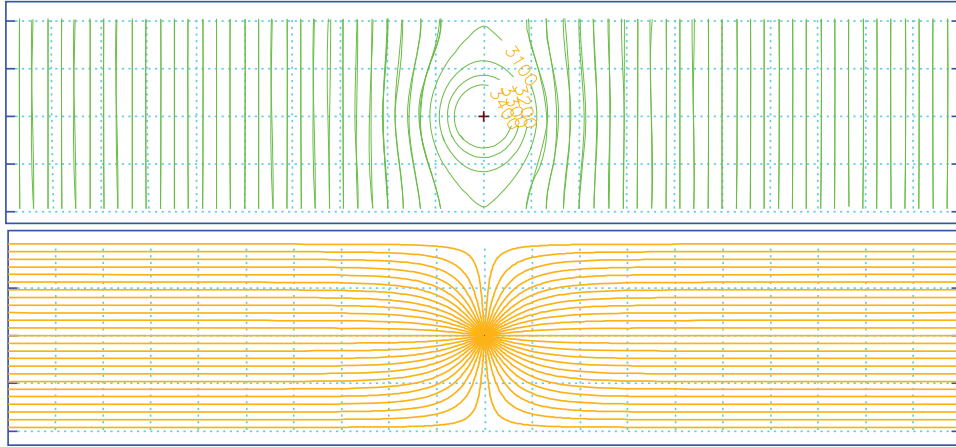


Figure 3: The electric potential (top) and field lines (bottom) as calculated for the geometry of an “electrodeless” drift chamber using the computer program GARFIELD [8].

The (total) charge density on the wire can therefore be written

$$\lambda = \frac{abV_0}{4\pi b_1 b_2 (1 + K)} \quad (V_1 = V_2 = 0). \quad (9)$$

The term $4\pi\lambda b_1 b_2 / ab$ of eq. (7) corresponds to a sheet of charge density λ/a at $y = 0$, which is at distances b_1 and b_2 from grounded planes. For such a sheet, Gauss’ law determines

electric fields in regions 1 ($-b_1 < y < 0$) and 2 ($0 < y < b_2$) to be

$$E_{1,\text{sheet}} = -\frac{4\pi\lambda b_2}{ab}, \quad \text{and} \quad E_{2,\text{sheet}} = \frac{4\pi\lambda b_1}{ab} \quad (V_1 = V_2 = 0), \quad (10)$$

so $V_{0,\text{sheet}} = -E_1 b_1 = E_2 b_2 = 4\pi\lambda b_1 b_2 / ab$. The charge densities on the two sides of the sheet would be $\sigma_{1,2} = \mp E_{1,2,\text{sheet}} / 4\pi$, which sum to the total charge density $\sigma = \lambda/a$ that was introduced in eq. (2). However, $\sigma_1 \neq \sigma_2$ if $b_1 \neq b_2$. This suggests that the charge distribution on the wire is no longer azimuthally symmetric if $b_1 \neq b_2$.

2.1.1 Angular Distribution of Charge on a Wire

To analyze the azimuthal dependence of the charge distribution on the wire, we consider the fields in the device to be the sum of a uniform background field E_B plus a field $E_0(x, y)$ that is antisymmetric about the grid, *i.e.*, antisymmetric in y . That is,

$$E_1(x, -y) = E_B - E_0(x, y), \quad E_2(x, y) = E_B + E_0(x, y). \quad (11)$$

For $|y| \gtrsim a$ all of these fields become uniform, with values corresponding to the grid being transformed into a sheet, so we can write

$$E_{1,\text{sheet}} = E_B - E_{0,\text{sheet}}, \quad E_{2,\text{sheet}} = E_B + E_{0,\text{sheet}}. \quad (12)$$

Using (10) we find,

$$E_B = \frac{E_{1,\text{sheet}} + E_{2,\text{sheet}}}{2} = \frac{2\pi\lambda(b_1 - b_2)}{ab}, \quad (13)$$

$$E_{0,\text{sheet}} = \frac{E_{2,\text{sheet}} - E_{1,\text{sheet}}}{2} = \frac{2\pi\lambda}{a} = 2\pi\sigma. \quad (14)$$

The antisymmetric part of the field, E_0 , is essentially identical to that of the isolated grid, considered in sec. 1. Hence, the charge distribution σ_0 on the wire corresponding to this field is azimuthally symmetric, with value

$$\sigma_0 = \frac{\lambda}{2\pi r_0}. \quad (15)$$

The uniform background field E_B induces no net charge on the conducting wire, but does lead to a dipolar charge distribution. This is described by the well-known solution to the problem of a grounded conducting wire in an otherwise uniform background field. The potential has the form

$$V_B = -E_B \left(r - \frac{r_0^2}{r} \right) \sin \theta, \quad (16)$$

where angle θ is measured from the x -axis. The charge distribution σ_B induced on the wire by field E_B is therefore

$$\sigma_B = \frac{E_{B,r}(r_0)}{4\pi} = -\frac{1}{4\pi} \frac{\partial V_B(r_0)}{\partial r} = \frac{E_B \sin \theta}{2\pi} = \frac{\lambda(b_1 - b_2) \sin \theta}{ab}. \quad (17)$$

The total distribution of charge on the wire is the sum of eqs. (15) and (17),

$$\sigma_{\text{wire}}(\theta) = \frac{\lambda}{2\pi r_0} \left(1 + \frac{r_0 E_B \sin \theta}{\lambda} \right) = \frac{\lambda}{2\pi r_0} \left(1 + \frac{2\pi r_0 (b_1 - b_2) \sin \theta}{a b} \right). \quad (18)$$

Since $(b_1 - b_2)/b \geq -1$, the charge distribution $\sigma_{\text{wire}}(\theta)$ has the same sign as λ for all angles. The charges on the grounded cathodes have the opposite sign to λ , and all field lines flow from the cathodes to the grid wires (or all lines flow from the grid to the cathodes).

2.2 Arbitrary Potentials on the Electrodes

The general case, with potential V_1 at $y = -b_1$ and V_2 at $y = b_2$, can be built up from the case of grounded cathodes by adding the linearly varying potential,

$$\Delta V = V_1 \frac{b_2 - y}{b} + V_2 \frac{b_1 + y}{b}, \quad (19)$$

to that of eqs. (54)-(55). Combining eqs. (7) and (19), the potential on the wire of radius r_0 (at $y = 0$) is

$$V_0 \approx V_1 \frac{b_2}{b} + V_2 \frac{b_1}{b} + \frac{4\pi b_1 b_2 (1 + K)}{ab} \lambda, \quad (20)$$

which determines the (total) charge density λ to be

$$\lambda \approx \frac{a(V_0 b - V_1 b_2 - V_2 b_1)}{4\pi b_1 b_2 (1 + K)} = \frac{a}{4\pi(1 + K)} \left(\frac{V_0 - V_2}{b_2} - \frac{V_1 - V_0}{b_1} \right). \quad (21)$$

2.2.1 Fields Far from the Grid

Recall that if the grid is transformed into a continuous sheet then λ/a becomes the areal charge density. Equation (21) is consistent with this limit if we suppose that $a/2\pi r_0 \rightarrow 1$ for a sheet, in which case the logarithmic term K vanishes and $\lambda/a \rightarrow (E_2 - E_1)/4\pi$ with

$$E_{1,\text{sheet}} = \frac{V_1 - V_0}{b_1}, \quad \text{and} \quad E_{2,\text{sheet}} \rightarrow \frac{V_0 - V_2}{b_2}, \quad (22)$$

as expected from Gauss' law.

The electric fields in the regions 1 and 2 differ from their values (10) in the case of grounded cathodes (with charge λ on each wire) by the addition of the background field

$$E_B = \frac{V_1 - V_2}{b}, \quad (23)$$

due to the potential (20).

When electrode 0 is a wire grid, the values of the field strengths in regions 1 and 2 (away from the wires) are the sum of eqs. (10) and (23) with λ according to eq. (21),

$$E_1 = \frac{V_1 - V_2}{b} - \frac{4\pi \lambda b_2}{ab} \approx \frac{V_1 - V_0}{b_1} + \frac{b_2}{b} \left(\frac{V_0 - V_2}{b_2} - \frac{V_1 - V_0}{b_1} \right) \frac{K}{1 + K}, \quad (24)$$

$$E_2 = \frac{V_1 - V_2}{b} + \frac{4\pi \lambda b_1}{ab} \approx \frac{V_0 - V_2}{b_2} - \frac{b_1}{b} \left(\frac{V_0 - V_2}{b_2} - \frac{V_1 - V_0}{b_1} \right) \frac{K}{1 + K}. \quad (25)$$

If the grid is transformed into a sheet, the logarithmic constant K in eqs. (24) and (25) vanishes and the fields revert to the values (22), as expected.

These approximations hold only for $|y| \gtrsim a$ and $a \lesssim b_1, b_2$. In this regime, the fields E_1 and E_2 differ only slightly from their values when the grid is replaced by a sheet. If $E_2 > E_1$ then the bulk field E_1 in the presence of a grid is larger (and E_2 is smaller) than the fields (22) for a sheet. Of course, since the y -integral of the field E_1 must always equal $V_1 - V_0$, a larger field over most of the interval $-b_1 < y < 0$ implies that E_1 must be small (or negative) near $y = 0$.

2.2.2 Angular Distribution of Charge on a Wire

We can calculate the angular distribution of charge on a grid wire as was done in sec. 2.1.1. However, the “background” electric field that induces this angular distribution is not simply eq. (23) [due to potentials V_1 and V_2 on the cathodes], but the sum of this and eq. (13) [which is the uniform part of the field of a grid plus grounded cathodes]. Thus, for purposes of determining the angular distribution of charge on the wire, we write

$$E_B = \frac{V_1 - V_2}{b} + \frac{2\pi\lambda(b_1 - b_2)}{ab}. \quad (26)$$

As in eq. (18), we now find the angular distribution to be

$$\begin{aligned} \sigma_{\text{wire}}(\theta) &= \frac{\lambda}{2\pi r_0} + \frac{E_B \sin \theta}{2\pi} = \frac{V_1 - V_2}{2\pi b} \sin \theta + \frac{\lambda}{2\pi r_0} \left(1 + \frac{2\pi r_0}{a} \frac{(b_1 - b_2) \sin \theta}{b} \right) \\ &= \frac{V_1 - V_0}{b_1} \frac{b_1 \sin \theta}{2\pi b} + \frac{V_0 - V_2}{b_2} \frac{b_2 \sin \theta}{2\pi b} \\ &\quad + \frac{a}{8\pi^2 r_0 (1 + K)} \left(\frac{V_0 - V_2}{b_2} - \frac{V_1 - V_0}{b_1} \right) \left(1 + \frac{2\pi r_0}{a} \frac{(b_1 - b_2) \sin \theta}{b} \right) \\ &= \frac{V_0 - V_2}{b_2} \left[\frac{a}{8\pi^2 r_0 (1 + K)} \left(1 + \frac{2\pi r_0}{a} \frac{(b_1 - b_2) \sin \theta}{b} \right) + \frac{b_2 \sin \theta}{2\pi b} \right] \\ &\quad - \frac{V_1 - V_0}{b_1} \left[\frac{a}{8\pi^2 r_0 (1 + K)} \left(1 + \frac{2\pi r_0}{a} \frac{(b_1 - b_2) \sin \theta}{b} \right) - \frac{b_1 \sin \theta}{2\pi b} \right]. \quad (27) \end{aligned}$$

Unlike the case of a grid plus grounded cathodes, the distribution $\sigma_{\text{wire}}(\theta)$ can include both positive and negative charges. This permits grids be made effectively transparent to drifting electrons for a suitable range of potentials V_0, V_1 and V_2 .

2.2.3 Transparency of the Grid to Drifting Electrons

In other applications of grids to particle detectors, it is desired that ionization electrons that are created in region 1 drift into region 2 without being “captured” by the grid. Rather, the drifting electrons are to be collected at electrode 2. In this case, the grid should be “transparent” to the drifting electrons.

We see from the discussion in sec. 2.1.1 that the transparency is zero for the grid of an MWPC with grounded cathodes. This is, of course, desirable in that application, since the grid of an MWPC, rather than electrode 2, serves to collect the drifting electrons.

To make the grid completely transparent to electrons in region 1, none of the field lines that leave electrode 1 can end on the grid.¹ Therefore, the charge on the grid wires must have the same sign as the charge on electrode 1. The critical condition is that the point on a grid wire closest to electrode 1, *i.e.*, $\theta = -\pi/2$, have zero charge.

Requiring that $\sigma_{\text{wire}}(\theta = -\pi/2) = 0$ in eq. (27) we find,²

$$\begin{aligned} \frac{E_{2,\text{sheet}}}{E_{1,\text{sheet}}} &= \frac{\frac{V_0 - V_2}{b_2}}{\frac{V_1 - V_0}{b_1}} = \frac{1 - \frac{2\pi r_0}{a} \frac{(b_1 - b_2)}{b} + \frac{4\pi b_1 r_0 (1 + K)}{ab}}{1 - \frac{2\pi r_0}{a} \frac{(b_1 - b_2)}{b} - \frac{4\pi b_2 r_0 (1 + K)}{ab}} \\ &\approx 1 + \frac{4\pi r_0}{a} (1 + K) \quad (\text{full transparency}), \end{aligned} \quad (28)$$

where K is defined in eq. (8). For a detector where region 1 is much larger than region 2, and with wire spacing a equal to distance b_2 , this becomes³

$$\frac{E_{2,\text{sheet}}}{E_{1,\text{sheet}}} \approx 1 + \frac{4\pi r_0}{a} \left(1 + \frac{1}{2\pi} \ln \frac{a}{2\pi r_0} \right) \quad (a = b_2 \ll b_1). \quad (30)$$

A typical grid might have $a/2r_0 \approx 100$, so $\ln(a/2\pi r_0) \approx 3.5$, for which full transparency requires

$$\frac{E_{2,\text{sheet}}}{E_{1,\text{sheet}}} \approx 1.1 \quad (a = 200r_0 = b_2 \ll b_1). \quad (31)$$

2.2.4 From Full Transparency to Zero Transparency

It is sometimes desired to use a grid as a gate, changing the value of potential V_0 on the grid to a value such that the transparency is zero for electrons drifting from region 1. In this case, all field lines from region 1 must terminate on the grid.

A simple way to achieve this is to switch the grid to potential V_2 . Then there is no electric field in region 2, so all field lines in region 1 must end on the grid, as desired.

For example, if we operate with $V_2 = 0$ (to have the readout electronics on the collection electrode 2 at ground potential), then the condition (31) for full transparency for, say $b_1 = 100b_2$, is that $V_0 = V_1 b_2 / (1.07b_1 + b_2) \approx V_1 / 108$. Switching the small voltage $V_0 = V_1 / 108$ to ground is a relatively easy task.

¹This condition is necessary, but perhaps not quite sufficient, since the drifting electrons may not follow field lines if these curve too sharply near the grid. We follow the conventional wisdom in adopting this condition to obtain analytic results.

²Ref. [1] appears to claim that the critical ratio is simply $1 + 4\pi r_0 / a$. Equation (3.23) of [2] appears to be something like our form.

³H. Jostlein has proposed a configuration in which $a \ll b_1 \ll b_2$, in which case $K \approx 0$ and the criterion for full transparency is

$$\frac{E_{2,\text{sheet}}}{E_{1,\text{sheet}}} \approx 1 + \frac{4\pi r_0}{a} \quad (a \ll b_1 \ll b_2). \quad (29)$$

Jostlein's application is for a mesh grid, rather than a wire grid. In case of a mesh that is 80% open, $r_0/a = 0.1$, and $E_{2,\text{sheet}}/E_{1,\text{sheet}} \approx 2.25$.

2.2.5 Gain Grid at the End of a Long Drift Region

In some gaseous particle detectors it is desired to collect the ionization electrons on a grid after they have drifted across region 1, where the length b_1 of the drift region is large compared to the grid wire spacing a . Further, the electric field near a grid wire is to be so large that Townsend avalanches occur, thereby amplifying the signal due to the drifting electrons.

A basic configuration for this has a planar electrode at $y = -b_1$ at a large negative voltage ($V_1 < 0$), a grounded grid at $y = 0$ ($V_0 = 0$), and another planar electrode at $y = b_2 \approx a \ll b_1$ that is also at a negative voltage ($V_2 < 0$) to insure that all electrons drifting in region 1 are collected on the grid.

The field strength E_1 in the bulk of region 1 is chosen to have a specific value suitable for drifting electrons through the chamber gas. The electric field at the surface of a grid wire must have a large value to produce gain via Townsend avalanches. According to eq. (6), the field at the wire can be written

$$\begin{aligned} E_{\text{wire}} &= (E_2 - E_1) \frac{a}{2\pi r_0} \approx \left(\frac{V_0 - V_2}{b_2} - \frac{V_1 - V_0}{b_1} \right) \frac{a}{2\pi r_0 (1 + K)} \\ &\approx - \left(\frac{V_2}{a} + \frac{V_1}{b_1} \right) \frac{a}{2\pi r_0 (1 + K)}, \end{aligned} \quad (32)$$

where E_1 and E_2 are the fields (24)-(25) in the bulk of regions 1 and 2, K is defined in eq. (8), and the final form holds for the present example.

Even if V_1 must be held at a value such that a field of strength $V_1 a / 2\pi b_1 r_0 (1 + K)$ is too small to produce Townsend avalanches near the wire, voltage V_2 can be independently raised until the desired gas gain is achieved. For example, if the desired gas gain is achieved when operating an MWPC with grounded cathodes at $b_1 = b_2 = a$ and wires of radius r at voltage V , then electric field at a wire of the MWPC is

$$E_{\text{MWPC wire}} \approx - \frac{V}{\pi r (1 + K_r)}, \quad (33)$$

The drift chamber under discussion can achieve this field on its wires with

$$V_2 \leq 2V \frac{r_0 (1 + K)}{r (1 + K_r)}, \quad (34)$$

for any choice of V_1 . If $r_0 = r$, then we need $V_2 \leq 2V$, etc.

Conversely, if the field strength $V_1 a / 2\pi b_1 r_0 (1 + K)$ is so large that the gain would be excessive in the drift chamber, the wire radius r_0 can be made larger than r and the gain reduced to an acceptable value. Voltage V_2 can then be varied to provide fine tuning of the gas gain.

3 Appendix 1: Potential of a Single Grid Plane

(From Ph501, Problem Set 3 [4].)

A grid of infinitely long wires is located in the (x, y) plane at $y = 0$, $x = \pm na$, $n = 0, 1, 2, \dots$, as shown in Fig. 1. Each line carries charge λ per unit length.

This problem is 2-dimensional, and is well described in rectangular coordinates (x, y) . We try separation of variables:

$$V(x, y) = \sum X(x)Y(y). \quad (35)$$

Away from the surface $y = 0$, Laplace's equation, $\nabla^2 V = 0$, holds, so one of X and Y can be oscillatory and the other exponential. The X functions must be periodic with period a , and symmetric about $x = 0$. This suggests that we choose

$$X_n(x) = \cos k_n x, \quad \text{with} \quad k_n = \frac{2n\pi}{a}. \quad (36)$$

We first consider the regions $y > 0$ and $y < 0$ separately, and then match the solutions at the boundary. The Y functions are exponential, and should vanish far from the plane $y = 0$. Hence we consider

$$Y_n(y) = \begin{cases} e^{-k_n y}, & y > 0, \\ e^{k_n y}, & y < 0. \end{cases} \quad (37)$$

However, we must remember that the case of index $n = 0$ is special in that the separated equations are $X_0'' = 0 = Y_0''$, so that we can have $X_0 = 1$ or x , and $Y_0 = 1$ or y . In the present case, $X_0 = 1$ is the natural extension of (36) for nonzero n , so we conclude that $Y_0 = \pm y$ is the right choice; otherwise $X_0 Y_0 = 1$, which is trivial. Then the potential $V = \pm y$ will be associated with a constant electric field in the y direction, which is to be expected far from the grid of wires.

Combining X and Y , our series solution thus far is

$$V(x, y) = \begin{cases} a_0 y + \sum_{n>0} a_n \cos \frac{2n\pi x}{a} e^{-2n\pi y/a}, & y > 0, \\ -a_0 y + \sum_{n>0} a_n \cos \frac{2n\pi x}{a} e^{2n\pi y/a}, & y < 0, \end{cases} \quad (38)$$

where we have used continuity of the potential at $y = 0$ to use the same a_n for both $y > 0$ and $y < 0$. Note, however, the sign change for a_0 , corresponding to the constant electric field that points away from the wire plane.

At the boundary, $y = 0$, the surface charge density is

$$\begin{aligned} \sigma &= \lambda \sum_n \delta(x - na) = \frac{1}{4\pi} (E_y(0^+) - E_y(0^-)) = \frac{1}{4\pi} \left(-\frac{\partial\phi(x, 0^+)}{\partial y} + \frac{\partial\phi(x, 0^-)}{\partial y} \right) \\ &= -\frac{a_0}{2\pi} + \frac{1}{a} \sum_n n a_n \cos \frac{2n\pi x}{a}. \end{aligned} \quad (39)$$

We evaluate the a_n by considering the interval $[-a/2 < x < a/2]$. Multiplying by $\cos(2n\pi x/a)$ and integrating, we find

$$a_0 = -\frac{2\pi\lambda}{a}, \quad \text{and} \quad a_n = \frac{2\lambda}{n}. \quad (40)$$

The potential is then,

$$V(x, y) = -\frac{2\pi\lambda|y|}{a} + 2\lambda \sum_{n>0} \frac{1}{n} \cos \frac{2n\pi x}{a} e^{-2n\pi|y|/a}. \quad (41)$$

To sum the series, we write it as

$$\begin{aligned}
V(x, y) &= -\frac{2\pi\lambda|y|}{a} + 2\lambda Re \sum_{n>0} \frac{1}{n} e^{2n\pi x/a} e^{-2n\pi|y|/a} \\
&= -\frac{2\pi\lambda|y|}{a} + 2\lambda Re \sum_{n>0} \frac{1}{n} (e^{2\pi i x/a} e^{-2\pi|y|/a})^n \\
&= -\frac{2\pi\lambda|y|}{a} - 2\lambda Re \ln(1 - z),
\end{aligned} \tag{42}$$

where

$$z = e^{2\pi i x/a} e^{-2\pi|y|/a}. \tag{43}$$

To take the real part, we note that if

$$\ln(1 - z) \equiv u + iv, \quad \text{then} \quad 1 - z = e^u e^{iv}, \quad |1 - z| = e^u, \tag{44}$$

and

$$\begin{aligned}
Re \ln(1 - z) &= u = \ln |1 - z| \\
&= \ln |1 - e^{-2\pi|y|/a} [\cos(2\pi x/a) + i \sin(2\pi x/a)]| \\
&= \ln \sqrt{1 - 2 \cos(2\pi x/a) e^{-2\pi|y|/a} + e^{-4\pi|y|/a}} \\
&= \frac{1}{2} \ln [1 - 2 \cos(2\pi x/a) e^{-2\pi|y|/a} + e^{-4\pi|y|/a}].
\end{aligned} \tag{45}$$

The potential is now

$$\begin{aligned}
V(x, y) &= -\lambda \ln e^{2\pi|y|/a} - \lambda \ln [1 - 2 \cos(2\pi x/a) e^{-2\pi|y|/a} + e^{-4\pi|y|/a}] \\
&= -\lambda \ln [e^{2\pi|y|/a} - 2 \cos(2\pi x/a) + e^{-2\pi|y|/a}] \\
&= -\lambda \ln \left[2 \cosh \frac{2\pi y}{a} - 2 \cos \frac{2\pi x}{a} \right]
\end{aligned} \tag{46}$$

This result can also be deduced by the use of functions of a complex variable [3].

For x, y small:

$$\cosh \frac{2\pi y}{a} - \cos \frac{2\pi x}{a} \approx 1 + \frac{1}{2} \left(\frac{2\pi y}{a} \right)^2 + \dots - 1 + \frac{1}{2} \left(\frac{2\pi x}{a} \right)^2 + \dots = \frac{1}{2} \left(\frac{2\pi r}{a} \right)^2 \tag{47}$$

where $r^2 = x^2 + y^2$. Thus, at small x, y ,

$$V(x, y) \rightarrow -2\lambda \ln \frac{2\pi r}{a}, \tag{48}$$

which is just the potential for an individual line charge λ . Close to each wire, the equipotentials are cylinders around this wire.

4 Appendix 2: Grid + Planar Cathodes

(Multiwire Proportional Chamber and “Electrodeless” Drift Chamber, from [5].)

Consider a unit cell of a wire grid with spacing a surrounded by a pair of conducting cathodes at distances b_1 and b_2 (where $b_1 + b_2 \equiv b$), as shown in Fig. 2.

If the side walls of the cell are dielectric, we have the configuration of the so-called “electrodeless” drift chamber.

If the unit cell shown in Fig. 2 is replicated so as to form an array of cells in x with period a , we have in the geometry of a multiwire proportional chamber (MWPC) with planar cathodes. Typically $b_1 = b_2 = b/2$.

Find the potential assuming that the electric field is parallel to the surfaces $x = \pm a/2$, that the cathodes are grounded, and that the wire carries charge λ per unit length. Generalize this solution to the case of potential V_1 on the lower cathode, V_2 on the upper cathode, and V_0 on the grid.

4.1 Wire On the x Miplane

We analyze the cell, shown in Fig. 2, in a coordinate system with its origin on the wire. Assuming grounded cathodes and that no electric field lines cross the surfaces $x = \pm a/2$, the boundary conditions on the outer surfaces are

$$V(x, -b_1) = V(x, b_2) = 0, \quad \frac{\partial V(-a/2, y)}{\partial x} = \frac{\partial V(a/2, y)}{\partial x} = 0, \quad (49)$$

We consider the cell to be divided into two regions, $y < 0$ and $y > 0$. The matching condition on the plane $y = 0$ follows from Gauss’s law:

$$-\frac{\partial V(x, 0^+)}{\partial y} + \frac{\partial V(x, 0^-)}{\partial y} = 4\pi\lambda\delta(x), \quad (50)$$

The boundary conditions (49) on the outer surfaces of the cell indicate that a suitable series expansion for the potential, continuous across $y = 0$, is

$$V(x, y > 0) = A_0 b_1 (b_2 - y) + \sum_{n=1}^{\infty} A_n \cos \frac{2n\pi x}{a} \sinh \frac{2n\pi(b_2 - y)}{a} \sinh \frac{2n\pi b_1}{a}, \quad (51)$$

$$V(x, y < 0) = A_0 b_2 (b_1 + y) + \sum_{n=1}^{\infty} A_n \cos \frac{2n\pi x}{a} \sinh \frac{2n\pi(b_1 + y)}{a} \sinh \frac{2n\pi b_2}{a}. \quad (52)$$

Using the matching condition (50) at $y = 0$ we find the coefficient A_n to be

$$A_0 = \frac{4\pi\lambda}{ab}, \quad A_n = \frac{2\lambda}{n \sinh \frac{2n\pi b}{a}}, \quad (53)$$

where $b = b_1 + b_2$. Hence, the potential can be written

$$V(x, y > 0) = \frac{4\pi\lambda b_1 (b_2 - y)}{ab} + 4\lambda \sum_{n=1}^{\infty} \frac{1}{n} \cos \frac{2n\pi x}{a} \sinh \frac{2n\pi(b_2 - y)}{a} \frac{\sinh \frac{2n\pi b_1}{a}}{\sinh \frac{2n\pi b}{a}}, \quad (54)$$

$$V(x, y < 0) = \frac{4\pi\lambda b_2 (b_1 + y)}{ab} + 4\lambda \sum_{n=1}^{\infty} \frac{1}{n} \cos \frac{2n\pi x}{a} \sinh \frac{2n\pi(b_1 + y)}{a} \frac{\sinh \frac{2n\pi b_2}{a}}{\sinh \frac{2n\pi b}{a}}. \quad (55)$$

When $b_1 = b_2 = b/2$, the potential simplifies to

$$V(x, y) = \frac{\pi\lambda b}{a} - \frac{2\pi\lambda|y|}{a} + 2\lambda \sum_{n=1}^{\infty} \frac{1}{n} \cos \frac{2n\pi x}{a} \frac{\sinh \frac{2n\pi(b/2-|y|)}{a}}{\cosh \frac{n\pi b}{a}} \quad (\text{origin at the wire}). \quad (56)$$

For $a \ll b$, eq. (56) further simplifies to

$$V(x, y) \approx -\frac{2\pi\lambda|y|}{a} + 2\lambda \sum_{n=1}^{\infty} \frac{1}{n} \cos \frac{2n\pi x}{a} e^{-2n\pi|y|/a} \quad (\text{origin at the wire}), \quad (57)$$

neglecting the constant term $\pi\lambda b/a$, which then agrees with eq. (41) (and hence the closed form (46) also) of Appendix 1.

Apparently, the potential (56) can be expressed in ‘‘closed form’’ using Jacobian elliptic functions [6, 7], although it is not clear this has much practical advantage.

Except near $y = 0$, the exponential terms in eqs. (54)-(57) are small. So over most of the cell the potential varies linearly with y , and the electric field is parallel to the y axis. The field strength is $\pm 2\pi q/a$, as if the charge q were uniformly distributed over the plane ($|x| < a/2, 0$). For $x \approx 0, y \approx 0$ the equipotentials become cylinders around the wire, as shown in Fig. 3. This is, of course, the desirable field configuration for a drift chamber. .

The potential at the origin diverges. But, of course, a physical realization of a wire chamber involves a wire of finite radius r_0 . We can estimate the potential at the surface of the wire at position (x, y) , where $x^2 + y^2 = r_0^2 \ll a, b$, using eq. (56):

$$\begin{aligned} V_{\text{wire}} &= V(x > 0, y) \approx \frac{\pi\lambda b}{a} + 2\lambda \sum_{n=1}^{\infty} \cos \frac{2n\pi x}{a} \frac{\tanh \frac{2n\pi b}{2a} \cosh \frac{2n\pi y}{a} - \sinh \frac{2n\pi y}{a}}{n} \\ &\approx \frac{\pi\lambda b}{a} + 2\lambda Re \sum_{n=1}^{\infty} e^{2n\pi i x/a} \frac{\cosh \frac{2n\pi y}{a} - \sinh \frac{2n\pi y}{a}}{n} \\ &= \frac{\pi\lambda b}{a} + 2\lambda Re \sum_{n=1}^{\infty} \frac{e^{-2n\pi y/a} e^{2n\pi i x/a}}{n} = \frac{\pi\lambda b}{a} + 2\lambda Re \sum_{n=1}^{\infty} \frac{[e^{-2\pi(y-ix)/a}]^n}{n} \\ &= \frac{\pi\lambda b}{a} - 2\lambda Re \ln [1 - e^{-2\pi(y-ix)/a}]. \end{aligned} \quad (58)$$

Then writing $\ln [1 - e^{-2\pi(y-ix)/a}] = u + iv$ we have

$$e^{u+iv} = e^u \cos v + ie^u \sin v = 1 - e^{-2\pi(y-ix)/a} = 1 - e^{-2\pi y/a} \cos \frac{2\pi x}{a} + ie^{-2\pi y/a} \sin \frac{2\pi x}{a}, \quad (59)$$

$$\begin{aligned} e^{2u} &= \left(1 - e^{-2\pi y/a} \cos \frac{2\pi x}{a}\right)^2 + e^{-4\pi y/a} \sin^2 \frac{2\pi x}{a} = \left(1 - 2e^{-2\pi y/a} \cos \frac{2\pi x}{a} + e^{-4\pi y/a}\right) \\ &\approx 1 - 2 \left[1 - \frac{2\pi y}{a} + \frac{1}{2} \left(\frac{2\pi y}{a}\right)^2\right] \left[1 - \frac{1}{2} \left(\frac{2\pi x}{a}\right)^2\right] + 1 - \frac{4\pi y}{a} + \frac{1}{2} \left(\frac{4\pi y}{a}\right)^2 \\ &= \left(\frac{2\pi}{a}\right)^2 + \left(\frac{2\pi y}{a}\right)^2 = \left(\frac{2\pi r_0}{a}\right)^2, \end{aligned} \quad (60)$$

$$\operatorname{Re} \ln \left[1 - e^{-2\pi(y-ix)/a} \right] = u \approx \ln \frac{2\pi r_0}{a}, \quad (61)$$

and we finally have

$$V_{\text{wire}} \approx \frac{\pi\lambda b}{a} - 2\lambda \ln \frac{2\pi r_0}{a} = \frac{\pi\lambda b}{a} + 2\lambda \ln \frac{a}{2\pi r_0}. \quad (62)$$

The first term of this is just the “uniform” electric field $E_y = 2\pi\lambda/a$ multiplied by the distance $b/2$ between the wire and a ground plane. The second term is the same as the potential (48) for a wire on an isolated grid.

By comparing eqs. (54)-(55) with eq. (56), we see that the potential of the grid when $b_1 \neq b_2$ is given by

$$V_{\text{wire}} \approx \frac{4\pi\lambda b_1 b_2}{ab} + 2\lambda \ln \frac{a}{2\pi r_0}. \quad (63)$$

Again, the first term follows from Gauss’ law for a plane of charge density λ/a at distances b_1 and b_2 from grounded planes; the electric fields in regions 1 and 2 are then $E_{1,2} = \mp 4\pi\lambda b_{2,1}/ab$, so $V = -E_1 b_1 = E_2 b_2 = 4\pi\lambda b_1 b_2/ab$.

References

- [1] O. Bunemann *et al.*, *Design of Grid Ionization Chambers*, Can. J. Res. (Sec. A) **27**, 191 (1949),
http://puhep1.princeton.edu/~mcdonald/examples/detectors/bunemann_cjr_27_191_49.pdf
- [2] W. Blum and L. Rolandi, *Particle Detection With Drift Chambers* (Springer-Verlag, Berlin, 1994).
- [3] See, for example, J.C. Maxwell, *A Treatise on Electricity and Magnetism*, 3rd ed. (Dover reprint, New York, 1954), Vol. 1, p. 310.
- [4] K.T. McDonald, Princeton Ph501 Set 3,
<http://puhep1.princeton.edu/~mcdonald/examples/ph501set3.pdf>
- [5] C. Lu and K.T. McDonald, *The Electric Potential of Particle Detectors with Rectangular Cross Section* (Oct. 9, 2002),
<http://puhep1.princeton.edu/~mcdonald/examples/iarocci.pdf>
- [6] T. Tomitani, *Analysis of Potential Distribution in a Gaseous Counter of Rectangular Cross-Section*, Nucl. Instr. and Meth. **100**, 179 (1972),
http://puhep1.princeton.edu/~mcdonald/examples/EM/tomitani_nim_100_179_72.pdf
- [7] G.A. Erskine, *Electrostatic Problems in Multiwire Proportional Chambers*, Nucl. Instr. and Meth. **105**, 565 (1972),
http://puhep1.princeton.edu/~mcdonald/examples/EM/erskine_nim_105_565_72.pdf
- [8] GARFIELD, a computer program for simulation of gaseous detectors,
<http://consult.cern.ch/writeup/garfield/>